Journal of Catalysis **181,** 160–164 (1999)
Article ID jcat.1998.2281, available online at http://www.idealibrary.com on IDEAL®

RESEARCH NOTE

The Effect of SnO_2 Addition to Li/MgO Catalysts for the Oxidative Coupling of Methane

Katsutoshi Nagaoka, Takashi Karasuda, and Ken-ichi Aika[1]

Department of Environmental Chemistry and Engineering, Interdisciplinary Graduate School of Science & Engineering, Tokyo Institute of Technology, 4259 Nagatsuta, Midori-ku, Yokohama 226-8502, Japan

Received April 30, 1998; revised September 4, 1998; accepted September 15, 1998

The oxidative coupling of methane (OCM) to produce C_2 hydrocarbons has been a subject of intense research during the past decade and will be especially important when the oil price shall be high. There are two categories for the OCM, the redox system and the nonredox system. Examples of the former would be oxides of Sn, Pb, Sb, Bi, Tl, Cd, and Mn, which have been reported as effective catalysts since the studies of Keller and Bhasin (1). As the second category, irreducible oxides such as alkali earth metals and lanthanides have been found to be effective, especially when doped with alkali (2–4). Lattice defects have been proposed as the active center for these systems, for example, $[Li^+O^-]$ in MgO lattices (5) and O^- with a defect in MgO (6). The role of the catalyst and the reaction mechanism seem to be different among the two categories of catalysts: reducible or irreducible.

Korf *et al.* (7) have found that the activity and stability of the Li/MgO catalyst are improved by the addition of small amounts of the oxides of various transition and rare earth metals. Among a number of oxides tested (SnO_2, Dy_2O_3, TiO_2, and Tb_4O_7), SnO_2 was found to be the most promising promoter of the catalyst for the OCM. This system is interesting because two different types of oxides (reducible and irreducible) produce a synergism. Tin was found to prevent the evaporation of lithium (7, 8), improving the stability through making complex oxides (8).

Nibbelke *et al.* (9) have proposed that the effect of both lithium and tin (on MgO) is to increase the mobility of the bulk oxygen of the catalyst, resulting in an increase in the amount of exchangeable oxygen per unit BET surface area. Mallens *et al.* (10) have shown, by using the temporal analysis of products (TAP) setup, that the addition of tin increases the amount of reactive (uppermost lattice) oxygen. However, the cause of the synergism between tin and Li/MgO is still not clear.

[1] To whom correspondence should be addressed. Fax: +81-45-924-5441. E-mail: kenaika@chemenv.titech.ac.jp.

The aim of this work is to investigate the effect of SnO_2 addition to Li/MgO catalysts by using several characterization methods such as XPS, IR, and XRD. Activity measurements were carried out at 923 K, where the C_2 yield over Li/MgO catalyst was rather low. The effect of SnO_2 addition was analyzed by XPS with respect to the surface oxygen state and by XRD with respect to the bulk phase change.

Sn-Li/MgO catalysts were prepared by mixing MgO (Soekawa Chemicals) with SnO_2 (Kanto Chemical) and $LiNO_3$ (Kanto Chemical) in water. The content of tin was varied as 0, 1, 5, 10, 30, and 50 mol% against 100 mol% of MgO, while the lithium content was constant: 10 mol% (against 100 mol% of MgO). These materials are hereafter denoted as *x*Sn-Li/MgO, where *x* refers to the tin mol%. Appropriate amount of distilled water was added to the mixed powder to form paste, which were dried overnight at 373 K and then crushed and sieved to form grains of 8–10 mesh size.

The catalyst (0.2 g) was treated with He (20 ml/min) at 1073 K for 1 h, and the reactivity was measured at 923 K using a flow reactor (connected to a glass circulation system for BET measurement) under atmospheric pressure of the reactants (CH_4/Air/He = 16/20/14, 50 ml/min). Product analysis were started at 1 h after the reaction temperature was stabilized. Two on-line gas chromatographies were used: Shimadzu GC-8A FID with a Porapak Q column used to separate CH_4, C_2H_4, and C_2H_6 (higher hydrocarbons were not produced under these conditions); GL Science GC320 TCD with a WG-100 column used to separate CO, CO_2, N_2, and O_2. After the reaction, the reactant feed gas was replaced with He (20 ml/min) and the sample was cooled to room temperature, then the XRD (Rigaku Geigerflex) measurements were caried out.

The surface area (BET method with N_2) of the samples were 43.7, 44.6, 49.5, and 46.5 m^2/g for $x = 0$, $x = 1$, $x = 10$, and $x = 30$ of the *x*Sn-Li/MgO samples, respectively.

The samples were transferrd to the XPS (VG ESCALAB220i) chamber without exposure to atmosphere

0021-9517/99 $30.00

and subjected to measurements. The binding energy was calibrated, assuming the Mg 2*p* core level as 50.8 eV (11). Throughout the measurements the Mg 2*p* peak did not split and retained the same shape.

Sample wafers were placed in a quartz IR cell with NaCl windows connected to a closed circulation system and purged at 1073 K for 1 h. The background spectra were recorded by JASCO FT/IR-350 with 32 scans. Twenty torr of CO_2 were introduced into the system at room temperature and stood for 1 h. The sample wafers were evacuated at 923 K (the reaction temperature) and kept for 1 h. The IR spectra were recorded by the same instrument at room temperature with 32 scans.

CH_4 and O_2 conversions over *x*Sn-Li/MgO catalysts are shown in Fig. 1. The CH_4 conversion was increased by adding SnO_2 of 1 mol% ($x = 1$). Further addition of SnO_2 did not increase the conversion. While the O_2 conversion increased extensively with the addition of SnO_2 up to 50 mol%. The oxygen of SnO_2 is known to be active than that of Li/MgO (12), allowing the deep oxidation by the addition of SnO_2. The C_2 (C_2H_6, C_2H_4) selectivity and C_2 yield over *x*Sn-Li/MgO catalysts are shown in Fig. 2. The only byproducts were CO_x. Both the selectivity and the yield increased once with SnO_2 addition up to 1 mol%, then decreased abruptly at 5 mol% SnO_2, and finally increased slowly. Catalyst performances seemed to be divided into two regions (low *x* and high *x*) at $x = 5$.

After the evacuation at 1073 K, the O 1*s* and C 1*s* regions of the XP spectra of the *x*Sn-Li/MgO catalysts were measured and the results are shown in Fig. 3. Major O 1*s* peak appeared at 531.3–531.5 eV, which were assigned to

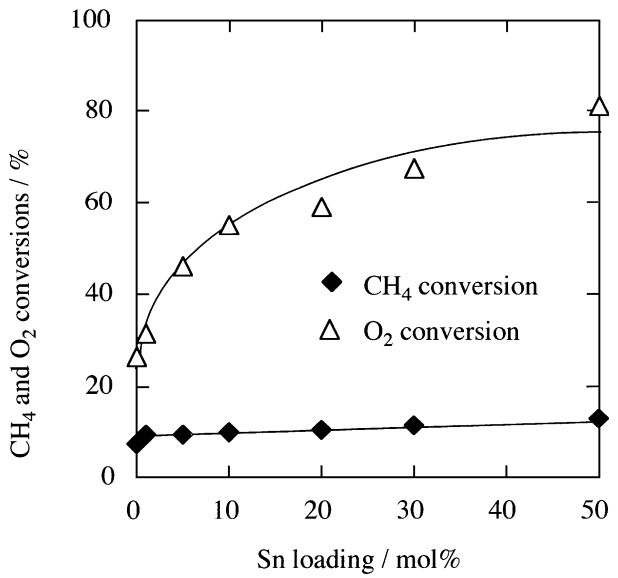

FIG. 1. Sn loading (*x*) dependence on CH_4 and O_2 conversions of OCM over *x*Sn-Li/MgO catalysts at 923 K.

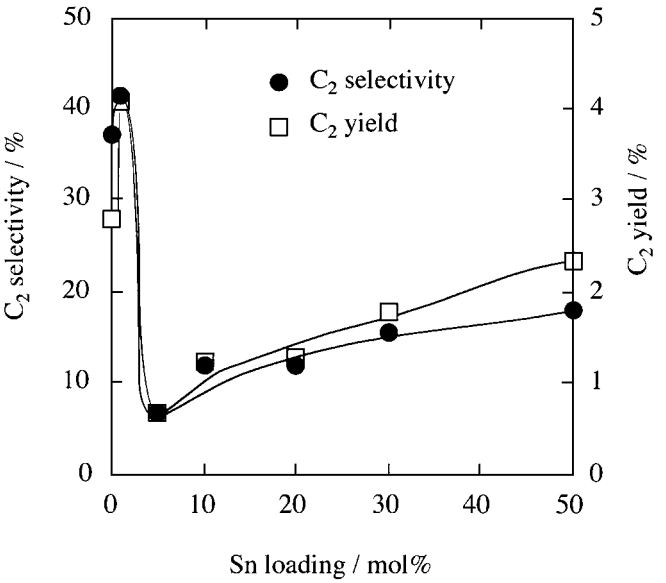

FIG. 2. Sn loading (*x*) dependence on C_2 selectivity and C_2 yield of OCM over *x*Sn-Li/MgO catalysts at 923 K.

O^{2-}. There was also a shoulder peak at the high binding energy side of the O 1*s* peak for the samples with $x = 0$, $x = 1$, $x = 5$, and $x = 10$. But the small shoulder for the sample with $x = 10$ disappeared after the reaction at 923 K. Peng *et al.* (11) have assigned the shoulder peak to the complication peaks of O^- and CO_3^{2-}. The nature of O^- shall be discussed in the later part of this work. To resolve the oxygen shoulder peak into two (O^- and CO_3^{2-}), carbon region was analyzed. Two kinds of the C 1*s* peaks were observed: 286.4–286.7 eV (amorphous contamination carbon) and 291.4–291.6 eV (CO_3^{2-} (11)). Figure 3 only shows the latter, which was not observed for the two samples with $x = 10$ and $x = 30$. Atomic sensitivity factors (13) were used to determine the atomic ratio of O^-/Mg and O^{2-}/Mg. The O 1*s* peak area of CO_3^{2-} was estimated from the C 1*s* peak of the CO_3^{2-} peak, thus, the O^- peak area of the O 1*s* shoulder peak was subsequently calculated. The ratio of O^-/O^{2-}, thus calculated, are shown for several samples in Table 1. The value of O^-/O^{2-} increased a litle when SnO_2 was added

TABLE 1

XPS Data about *x*Sn-Li/MgO Catalysts after the Pretreatment

Sn loading (x)/mol%	O 1*s* (O^-) B. E./eV	O^-/Mg[a]	O 1*s* (O^{2-}) B. E./eV	O^{2-}/Mg[a]	O^-/O^{2-}
0	533.7	0.38	531.3	1.51	0.25
1	533.4	0.49	531.3	1.47	0.34
10	533.6	0.17	531.3	1.22	0.14
30	nd	0	531.5	2.09	0

[a] Atomic ratio (surface).

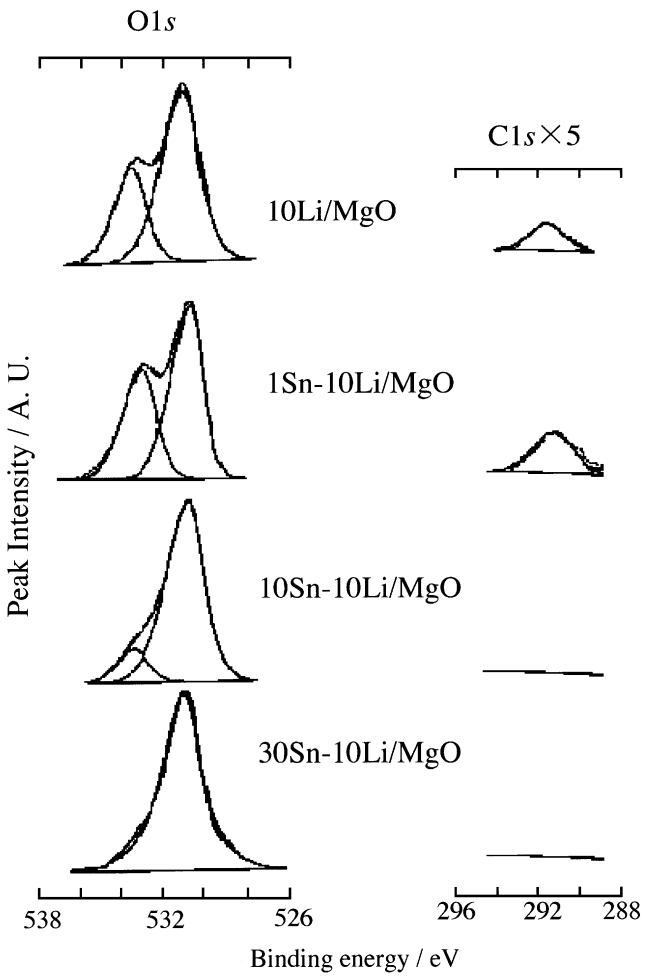

FIG. 3. O 1*s* and C 1*s* XP spectra over *x*Sn-Li/MgO catalysts after the pretreatment.

to 1 mol% ($x = 1$), while decreased with the further addition (Table 1). The atomic ratio of C 1*s* (of CO_3^{2-}) against Mg of the samples after the reaction are shown in Table 2. The surface carbon decreased drastically by the addition of SnO_2.

How CO_2 was left on the surface under the reaction conditions was also studied by FTIR. The FTIR spectra of the 923 K-CO_2-treated-surface were measured and are shown in Fig. 4. Peaks assigned to the carbonate appeared at 1409–1473 cm^{-1} for the samples with $x = 0$ and $x = 1$. Those assigned to Li_2CO_3 (14) could not be observed for the samples with $x = 10$ and $x = 30$. These results are corresponding well to the XPS data shown in Table 2.

In order to classify the SnO_2 effect, the bulk phase change was studied by XRD. Data for the sample with $x = 30$ under various conditions are shown in Fig. 5. The sample mixed with three components without pretreatment was found to be composed of two phases of $Mg(OH)_2$ and SnO_2. After pretreatment at 1073 K, the $Mg(OH)_2$ phase disappeared, and the MgO and $Li_2MgSn_2O_6$ phase appeared. All phases were not changed after reaction at 923 K. The phases observed with XRD for various *x*Sn-Li/MgO catalysts under various conditions are shown in Table 3. The Li_2CO_3 phase appeared after the reaction for a sample free of SnO_2 (Li/MgO). This phase disappeared when SnO_2 was added. Instead, for samples with SnO_2, a new complex oxide phase Li_2SnO_3 (15) appeared after pretreatment at 1073 K and remained after the reaction. This phase was changed to $Li_2MgSn_2O_6$ when the SnO_2 content was increased to 30 mol% ($x = 30$).

TABLE 2

XPS Data about *x*Sn-Li/MgO Catalysts after the Reaction

Sn loading (x)/mol%	C 1*s* (CO_3^{2-})	
	B. E./eV	C(CO_3^{2-})/Mg[a]
0	291.0	0.42
1	291.5	0.08
10	nd	0
30	nd	0

[a] Atomic ratio (surface).

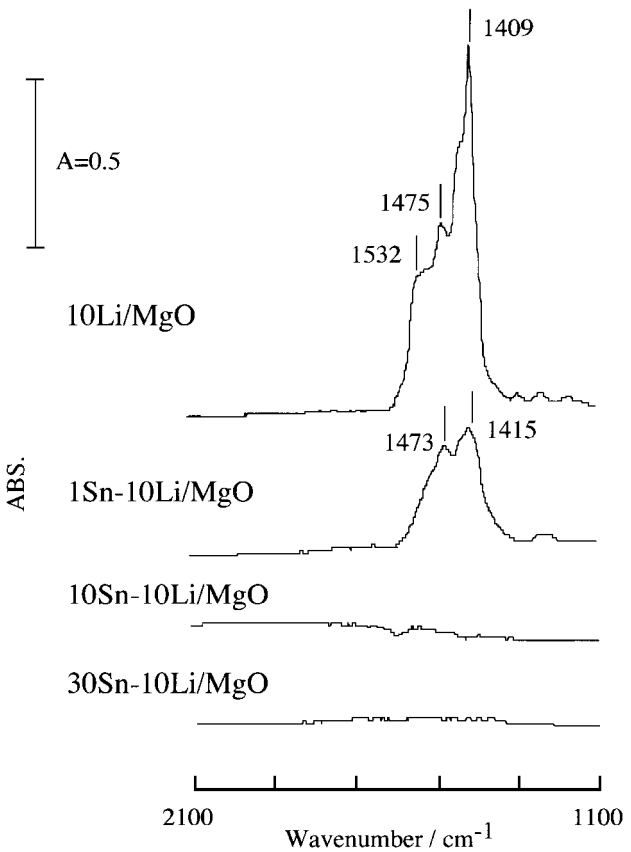

FIG. 4. FTIR spectra of adsorbed CO_2 at 300 K over *x*Sn-L/MgO catalysts, evacuated at 300 K and then temperature increased to 923 K.

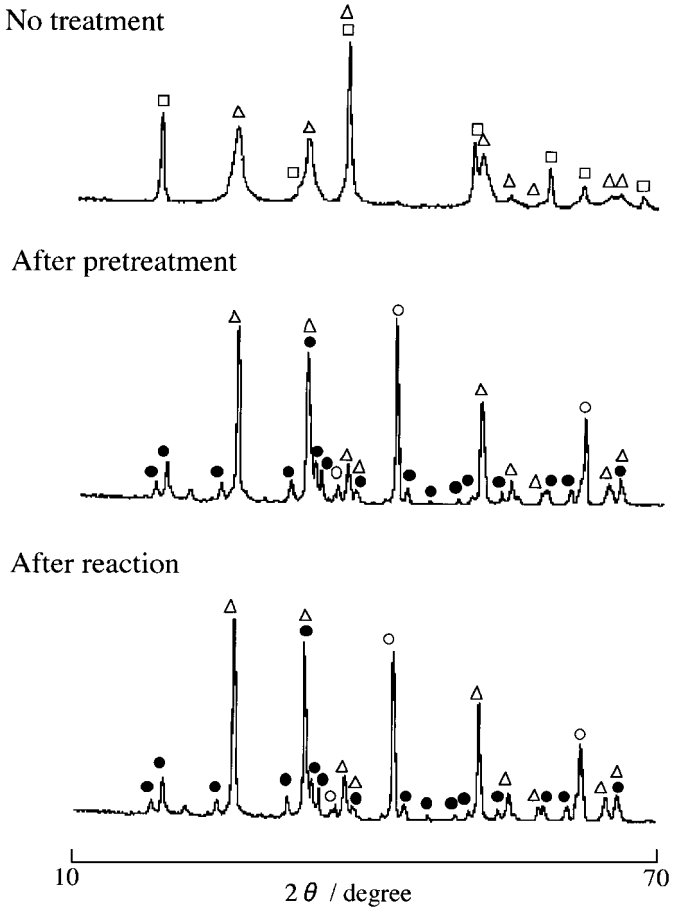

FIG. 5. XRD patterns over 30 Sn-Li/MgO catalysts in various conditions: ○, MgO; △, SnO_2; □, $Mg(OH)_2$; ●, $Li_2MgSn_2O_6$.

The shoulder peak of O 1*s* in the XP spectra in Fig. 3 was tentatively identified as O^- (11), and the relative amounts were estimated (Table 1). However, the nature of this state is quite different from O^- species with defects produced from N_2O on MgO with UV irradiation which can be detected by ESR (16). After CH_4 was introduced to the Li/MgO sample at room temperature after 1073 K pretreatment, the IR spectra were measured. However, no peak assignable to any surface product was observed in this study. On the other hand, IR investigations have shown that O^- on UV-activated MgO reacts with CH_4 at room temperature (16, 17) and turns to methoxide (17). Although the ESR spectra were not observable for the samples in this study, O^- on UV-activated MgO was observable with ESR (16, 17). Also the surface of the present sample was found to be much less reactive than the UV-activated one. Thus, the species identified as O^- of the present study should not have the same surface structure as the O^- species on UV activated surface. Thus surface O^- in this study might be interacting with nearby O^{2-}, mixing electrons with them and somehow becoming less reactive. Nevertheless, such a structure having electron-deficient-oxide-ions (O^-) must be closely linked to the OCM selectivity. As has been compared in Fig. 2 and Table 1, the C_2 yield and O^- concentration are closely related. Peng *et al.* (11) have also reported that CH_4 conversion is related to the area of the shoulder peak of O 1*s* for Li/MgO in the OCM.

The BET data (Experimental section) indicates that all catalysts have much the same specific surface areas. So the atomic ratio of the O^- species against O^{2-} (Table 1) is a suitable index of the active site of the OCM reaction.

The XPS (Table 2), IR (Fig. 4), and XRD (Table 3) data indicate that Li_2CO_3 is formed from the CO_2 and Li_2O produced on the surface and that the addition of SnO_2 decreases the amount of Li_2CO_3. When Li_2CO_3 exists in sufficient amounts on the surface, it decreases the active center $[Li^+O^-]$ of the OCM reaction (10, 14, 18). The decrease in Li_2CO_3 (restoration of Li^+O^- center) may be attributed to the formation of other complex oxides which contain lithium (Table 3). But the Li_2CO_3 (after the reaction) decreased drastically only when 1 mol% of SnO_2 was added (Table 2). Thus, Li_2SnO_3 formation is considered to stabilize the rest of the lithium (not as Li_2CO_3) as $[Li^+O^-]$. After all, the presence of tin seems to retard the formation of Li_2CO_3 which might cover the catalyst surface and to keep lithium as a form of Li_2SnO_3 or $[Li^+O^-]$. The loss of lithium has been shown to be prevented by the addition of SnO_2 (7, 8). The Li_2SnO_3 phase may be stable at high temperature to keep sufficient $[Li^+O^-]$ when SnO_2 is added to 1 mol%. This must be the reason why CH_4 conversion (Fig. 1) and C_2 selectivity (Fig. 2) are high for this sample.

For catalysts involving SnO_2, complex oxides were formed after 1073 K pretreatment: a binary oxide for the sample with low SnO_2 content and a tertiary oxide for that with high SnO_2 content (Fig. 5 and Table 3). The present

TABLE 3

Phase Identification of xSn-Li/MgO Catalysts by XRD

Sn loading (x)/mol%	No treatment	After pretreatment	After reaction
0	$Mg(OH)_2$	MgO	MgO, Li_2CO_3
1	$Mg(OH)_2$, SnO_2	MgO, Li_2SnO_3	MgO, Li_2SnO_3
10	$Mg(OH)_2$, SnO_2	MgO, SnO_2, Li_2SnO_3	MgO, SnO_2, Li_2SnO_3
30	$Mg(OH)_2$, SnO_2	MgO, SnO_2, $Li_2MgSn_2O_6$	MgO, SnO_2, $Li_2MgSn_2O_6$

authors identified these as $Li_2MgSn_2O_6$ in this study, while Hoogendam *et al.* proposed a different oxide, $Li_2Mg_3SnO_6$ (8). The difference may be attributed to differences in the procedures of pretreatment. They (8) calcined the sample at 1123 K, but our samples were treated under He at 1073 K.

As we have shown in Table 1, O^- was decreased by the further addition of SnO_2 over 1 mol%. The small amount of O^- for sample with $x = 10$ disappeared after the reaction at 923 K. We speculate that $[Li^+O^-]$ can co-exist with Li_2SnO_3 (and with Li_2CO_3) when a small amount of SnO_2 is added but that SnO_2 tends to include all of the lithium and destroy the $[Li^+O^-]$ or $[O^-Mg^{2+}O^-]$ structure when a large amount of SnO_2 is added. This may be the reason why the addition of SnO_2 more than 1 mol% suddenly decreases the C_2 selectivity (Fig. 2).

When the SnO_2 content is lower than 1 mol%, the C_2 selectivity is quite high and the surface is dense in electron-deficient-surface-oxide-ions (O^-), which is suggested to be the major active center of these samples. On the other hand, for the sample with SnO_2 more than 10 mol%, where O^- was not observed after the reaction at 923 K, the C_2 selectivity increased again slowly according to the addition of SnO_2. This suggests that the active center for the OCM is the redox oxide, i.e. O^{2-} of complex oxides, as shown in previous papers (1, 19). Here, the reaction may proceed by a redox cycle between Sn^{4+} and Sn^{2+}.

Two kinds of active centers for *x*Sn-Li/MgO in the OCM are suggested. One is thought to be electron-deficient-surface-oxide-ion (O^-), which is generated when small amounts of SnO_2 (less than 1 mol%) are added to Li/MgO catalysts. The other is O^{2-} of the complex oxide containing Sn, which is formed by the addition of a large amount of SnO_2. The reaction of O^{2-} should perform the redox cycle between Sn^{4+} and Sn^{2+}. Addition of SnO_2 to Li/MgO catalysts decreases the formation of Li_2CO_3 which covers the catalyst surface.

REFERENCES

1. Keller, G. E., and Bhasin, M. M., *J. Catal.* **73**, 9 (1982).
2. Ito, T., Wang, J.-X., Lin, C.-H., and Lunsford, J. H., *J. Amer. Chem. Soc.* **107**, 5062 (1985).
3. Ito, T., and Lunsford, J. H., *Nature(London)* **314**, 721 (1985).
4. Driscoll, D. J., Martir, W., Wang, J.-X., and Lunsford, J. H., *J. Amer. Chem. Soc.* **107**, 58 (1985).
5. Lee, J. S., and Oyama, S. T., *Catal. Rev. Sci. Eng.* **30**, 249 (1988).
6. Balint, I., and Aika, K., *J. Chem. Soc. Faraday Trans.* **91**, 1805 (1995).
7. Korf, S. J., Roos, J. A., Vertman, L. J., Van Ommen, J. G., and Ross, J. R. H., *Appl. Catal.* **56**, 119 (1989).
8. Hoogendam, G. C., van Keulen, A. N. J., Seshan, K., van Ommen, J. G., and Ross, J. R. H., *J. Chem. Soc., Chem. Commun.*, 1546 (1992).
9. Nibbelke, R. H., Scheerová, J., de Croon, M. H. J. M., and Marin, G. B., *J. Catal.* **156**, 106 (1995).
10. Mallens, E. P. J., Hoebink, J. H. B. J., and Marin, G. B., *J. Catal.* **160**, 222 (1996).
11. Peng, X. D., Richards, D. A., and Stair, P. C., *J. Catal.* **121**, 99 (1990).
12. Bielanski, A., and Harber, J., *Catal. Rev. Sci. Eng.* **19**, 1 (1979).
13. Jorgensen, C. K., and Berthou, H., *Faraday Discus. Chem. Soc.* **54**, 269 (1972).
14. Bhumkar, S. C., and Lobban, L. L., *Indus. Eng. Chem. Res.* **31**, 1856 (1992).
15. Ross, J. R. H., van Keulen, A. N. J., Hegarty, M. E. S., and Seshan, K., *Catal. Today* **30**, 193 (1996).
16. Aika, K., and Lunsford, J. H., *J. Phys. Chem.* 1393 (1977).
17. Goto, A., and Aika, K., *Bull. Chem. Soc. Jpn* **71**, 95 (1998).
18. Lunsford, J. H., Hinson, P. G., Rosynec, M. P., Shi, C., Xu, M., and Yang, X., *J. Catal.* **147**, 301 (1994).
19. Asami, K., Shikada, T., Fujimoto, K., and Tominaga, H., *Indus. Eng. Chem. Res.* **26**, 2348 (1987).